Citation: Sharafi S, Uchida TK. Stability of human balance during quiet stance with physiological and exoskeleton time delays. IEEE Robotics and Automation Letters 8(10): 6211–6218, 2023. doi: https://doi.org/10.1109/lra.2023.3304845.

# Stability of Human Balance During Quiet Stance With Physiological and Exoskeleton Time Delays

Shahin Sharafi[1] and Thomas K. Uchida[2]

***Abstract*—Human balance with exoskeleton assistance is studied using an inverted pendulum model, considering time delays in the muscle reflexes and the exoskeleton controller. The model includes two motors at the ankle joint whose maximum torques depend on the joint angle and angular velocity, reflecting the combined moment-generating capacity of all plantarflexor and dorsiflexor muscles. These "muscle-like" motors obey a proportional–derivative (PD) reflex control law where the angle and angular velocity of the ankle joint are subject to feedback delays. The stability of this system is analyzed using Galerkin projection to convert the governing neutral delay differential equation into a system of first-order ordinary differential equations (ODEs) and computing the eigenvalues of the ODE system. The stability analysis is then repeated with exoskeleton torques included at the ankle joint. The exoskeleton torques are assumed to obey a PD control law as well but with a unique state feedback delay. Stability charts reveal that the area of the stability region always increases as the exoskeleton delay decreases, but the area may decrease as the physiological delay decreases. The presented analytical framework enables investigation of the effect of control gains and time delays on the stability of a combined human–exoskeleton system.**

***Index Terms*—Human performance augmentation, physically assistive devices, prosthetics and exoskeletons.**

## I. Introduction

FALLING is the leading cause of injury in individuals aged 65 and older [1]. This demographic is expected to increase in size from 10% of the global population in 2022 to 16% in 2050 [2], representing a large projected increase in health care costs worldwide. A deeper understanding of human balance will enable the development of assistive devices that can predict loss of balance and prevent falls.

Several studies have investigated human balance using experimental techniques, gaining insight into the dynamics of our muscles (actuators) and reflexes (controllers). Sale et al. [3] characterized the strength of the ankle plantarflexor muscles (the calf muscles) as a function of ankle angle, finding that the peak ankle plantarflexion torque can be generated when the ankle is nearly fully dorsiflexed (i.e., with the toes pointed up), regardless of the angle of the knee. Marsh et al. [4] performed an analogous study on the dorsiflexor muscles, reporting that the peak ankle dorsiflexion torque can be generated when the ankle is plantarflexed by approximately 10 degrees. Bok et al. [5] investigated the effect of aging on ankle dynamics and postural stability. In older adults, decreases were observed in the strength of the ankle plantarflexor muscles and ankle eversion range of motion, while postural sway was observed to increase. Vette et al. [6] studied the time delay between muscle activation and ankle torque generation. They found that this electromechanical delay is approximately 0.3 seconds in healthy adults and must be considered when designing exoskeletons for individuals with spinal cord injury as this amount of delay is sufficient to threaten stability during quiet stance. Peterka [7] studied human postural control by quantifying responses when mechanical and sensory (visual) perturbations were applied to participants during quiet stance. Stiffness, damping, time delay, and other parameters related to postural control were estimated in various sensory environments and when subjected to various stimulus conditions.

Experimental studies of human movement provide valuable biological data, but simulations are not limited by the time and cost associated with collecting data. Simulations are particularly useful for studying hypothetical scenarios, such as virtual prototyping of exoskeletons, as well as potentially injurious scenarios, such as loss of balance. Many simulation-based studies of human balance during quiet stance employ a single inverted pendulum model as both systems have an upright equilibrium point that is inherently unstable and motion occurs predominantly at the ankle joint during quiet stance [8]. Verdaasdonk et al. [9] used an inverted pendulum model with plantarflexor and dorsiflexor muscles at the ankle joint to study how reflexes based on muscle length, velocity, and force feedback affect stable equilibria and limit cycles. They theorized that muscle stretch reflexes are the predominant control mechanism during stance. Masani et al. [10] used an inverted pendulum model with a proportional–derivative (PD) controller to represent the torque generated by muscle activity. They concluded that a PD controller is sufficient to control postural sway during quiet stance. Asai et al. [11] found that an intermittent PD controller captured features of postural sway that are not captured when a standard continuous PD controller is used. Insperger et al. [12], [13] used an inverted pendulum model with a torsional spring and torsional dashpot at the ankle joint to represent the passive stiffness and damping of the Achilles tendon and other biological structures, and either a PD controller or a proportional–derivative–acceleration (PDA)

Manuscript received: March 15, 2023; Revised: June 20, 2023; Accepted: July 29, 2023. This paper was recommended for publication by Editor Aniket Bera upon evaluation of the Associate Editor and Reviewers' comments. This work was supported by the Natural Sciences and Engineering Research Council of Canada (RGPIN-2019-05726 [T.K.U.]). The funders had no role in study design, data collection and analysis, decision to publish, or preparation of the manuscript. *(Corresponding author: Thomas K. Uchida.)*

[1]Shahin Sharafi is with the Department of Mechanical Engineering, University of Ottawa, 161 Louis-Pasteur, Ottawa, Ontario, K1N 6N5, Canada. Shahin.Sharafi@uottawa.ca

[2]Thomas K. Uchida is with the Department of Mechanical Engineering, University of Ottawa, 161 Louis-Pasteur, Ottawa, Ontario, K1N 6N5, Canada. tuchida@uottawa.ca

Digital Object Identifier (DOI): see top of this page.

controller to represent the torque generated by muscle activity. Stability boundaries were computed analytically. Insperger et al. found that the PDA controller resulted in a greater stability margin than the PD controller and was able to stabilize systems with larger feedback delays. Balogh et al. [14] investigated the stability of an inverted pendulum with a detuned PDA controller—that is, where the proportional, derivative, and acceleration feedback signals have different delays. They found that detuning the controller can improve stability, increasing the maximum tolerable feedback delay. Zelei et al. [15] used an inverted pendulum model with delayed state feedback, complemented with experiments, to study the response of the body to perturbations during quiet stance. They found that the experimentally observed response to a large perturbation is an optimal compromise between the speed of recovery and robustness to the perturbation. Milton et al. [16] used an experimental approach to study an inverted pendulum with delayed state feedback, stressing the importance of considering time delays in the study of human balance. Several studies have investigated balance specifically in individuals with movement disorders, including individuals with spinal cord injury [17], paraplegia [18], and stroke [19].

Time-delay systems are systems whose state derivatives depend explicitly on past states. The dynamics of such systems are governed by delay differential equations (DDEs), which can pose analytical challenges due to their nonlinear behaviour. One approach to analyzing DDE systems is to first convert them into a system of partial differential equations (PDEs), then use Galerkin projection to approximate the PDE system as a system of ordinary differential equations (ODEs). The resulting ODE system can then be analyzed using traditional methods. Vyasarayani [20], [21] used this strategy to study neutral and higher-order DDEs. Kandala et al. used Galerkin approximation to perform pole placement for second-order DDEs [22], [23] and to obtain the characteristic roots of DDE systems [24]. Ahsan et al. [25] presented a strategy to embed the boundary conditions into the PDE; the resulting PDE is free of separate boundary conditions and can be approximated using Galerkin projection. DDEs with time-periodic coefficients and time-periodic delays were studied by Sadath and Vyasarayani [26] and Ahsan et al. [27]. These theoretical developments were applied by Ahsan et al. [28] to study single- and double-pendulum models of human balance. Ahsan et al. found that PDA feedback generally results in larger stability margins than PD control, with some exceptions.

The stability of time-delay systems is especially pertinent to the development of exoskeletons for preventing falls in elderly individuals. Exoskeletons can deliver assistive torques to the body to compensate for the decreases in muscle strength [29] and increases in muscle reflex delays [30] observed in elderly individuals. For example, Kong and Jeon [31] presented an exoskeleton that provides assistance at the hip, knee, and ankle joints. Time delays due to sensing, computing, actuation, and force transmission is a challenge in the control of lower-limb exoskeletons. Ding et al. [32] proposed a strategy to control a walking-assist exoskeleton that avoids time delays by anticipating the ground reaction forces and thus predicting the progression through the gait cycle. Farkhatdinov et al. [33] demonstrated that a lower-limb exoskeleton can potentially increase muscle activity during quiet stance as the wearer reacts to the application of the assistive torques. This result highlights the importance of considering time delays in the controller design as well as the complex interaction between the biological and mechatronic systems.

In this work, we investigate the stability of human balance during quiet stance when assisted by an exoskeleton at the ankle. We use a single inverted pendulum model and consider physiological time delays as well as time delays in the exoskeleton controller. We use the Galerkin approximation method with Lagrange multipliers for imposing the boundary conditions and verify our numerical results through comparison to previous studies. This technique is then applied to a biomechanical model of stance in the sagittal plane, where an actuator at the ankle is used to generate the active torques that are applied by all muscles crossing the joint. Muscle activity is assumed to depend on the angle and angular velocity of the ankle joint [34], [35]. The stability of the unassisted human model is analyzed considering muscle reflex time delays. We then add a PD controller with state feedback delay to model the torques applied by an idealized exoskeleton, considering a unique time delay for the exoskeleton, and assess the stability of the assisted human model. The efficacy of PD-controlled exoskeletons has been demonstrated in experiments on maintaining human balance following a perturbation [18]. We demonstrate that smaller exoskeleton time delays result in larger regions of stability in parameter space, indicating a greater ability to maintain human balance. However, our results indicate that smaller physiological time delays do not necessarily lead to larger stability regions.

## II. Methods

The inverted pendulum model of quiet stance and the Galerkin approximation method are presented in Sections II-A and II-B, respectively. In Section II-C, we add muscles to the inverted pendulum model to include the dependence of muscle moments on the angle and angular velocity of the ankle joint. An idealized exoskeleton under PD control with delayed feedback is added to the model in Section II-D.

### A. Inverted Pendulum Model of Quiet Stance

The inverted pendulum model is shown in Fig. 1 and is governed by the following second-order neutral DDE:

$$\ddot{\theta}(t) + \alpha\dot{\theta}(t) + \beta\theta(t) = K_{\mathrm{pb}}\theta(t-\tau_{\mathrm{b}}) + K_{\mathrm{db}}\dot{\theta}(t-\tau_{\mathrm{b}}) + K_{\mathrm{ab}}\ddot{\theta}(t-\tau_{\mathrm{b}}), \quad (1)$$

where $\theta(t)$ is the angle of the pendulum relative to vertical, $\tau_{\mathrm{b}}$ is the delay of the biological system, and the gains of a generic PDA controller are $K_{\mathrm{pb}}$, $K_{\mathrm{db}}$, and $K_{\mathrm{ab}}$. Parameters $\alpha = \frac{1}{J}b_t$ and $\beta = \frac{1}{J}\left(mg\ell - k_t\right)$, where $m$ and $\ell$ are the mass and length of the pendulum, $J$ is the inertia of the pendulum about the ankle joint, $g$ is the gravitational acceleration, and the passive ankle torques applied by the muscles and other biological structures are represented by a torsional spring of stiffness $k_t$ and a torsional dashpot with damping coefficient

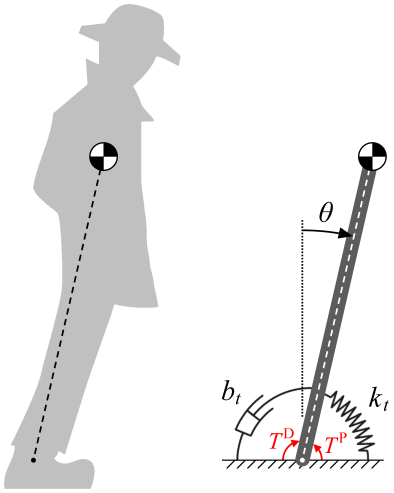


Fig. 1. Single inverted pendulum model of quiet stance in the sagittal plane.

$b_t$. We define state variables $z_1(t) = \theta(t)$ and $z_2(t) = \dot{\theta}(t)$, and write (1) in state-space form as follows:

$$\dot{z}_1(t) = f_1(t) = z_2(t), \tag{2a}$$
$$\dot{z}_2(t) = f_2(t) = -\beta z_1(t) - \alpha z_2(t) + K_{\mathrm{pb}} z_1(t-\tau_{\mathrm{b}}) + K_{\mathrm{db}} z_2(t-\tau_{\mathrm{b}}) + K_{\mathrm{ab}} \dot{z}_2(t-\tau_{\mathrm{b}}). \tag{2b}$$

### B. Galerkin Projection

We use the Galerkin approximation method with Lagrange multipliers to impose the boundary conditions. We begin by introducing the following transformation assuming a minimal set of independent generalized coordinates [20]:

$$y_i(s,t) = z_i(s+t), \quad i = 1, 2, \tag{3}$$

where

$$y_i(s,t) = \phi^{\mathrm{T}}(s) a_i(t), \quad i = 1, 2. \tag{4}$$

In (4), $\phi(s) = [\phi_1(s), \phi_2(s), \ldots, \phi_N(s)]^{\mathrm{T}}$ are the basis functions, $N$ is the number of modes retained in the Galerkin approximation, and $a_i(t)$ are the time-dependent coordinates. In this work, we use shifted Legendre polynomials as basis functions, which have been shown to have good convergence properties in this context [28]. As shown by Vyasarayani [20], it follows from (3) that

$$\frac{\partial y_i(s,t)}{\partial t} = \frac{\partial y_i(s,t)}{\partial s}, \quad i = 1, 2. \tag{5}$$

Substituting (5) into (2), we obtain the following:

$$\frac{\partial y_1(0,t)}{\partial t} = z_2(t), \tag{6a}$$
$$\frac{\partial y_2(0,t)}{\partial t} = -\beta z_1(t) - \alpha z_2(t) + K_{\mathrm{pb}} z_1(t-\tau_{\mathrm{b}}) + K_{\mathrm{db}} z_2(t-\tau_{\mathrm{b}}) + K_{\mathrm{ab}} \dot{z}_2(t-\tau_{\mathrm{b}}). \tag{6b}$$

We now impose the velocity constraints by introducing Lagrange multipliers into (5):

$$\frac{\partial y_i(s,t)}{\partial t} = \frac{\partial y_i(s,t)}{\partial s} + \delta(s)\gamma_i(t), \quad i = 1, 2, \tag{7}$$

where $\delta(s)$ is the Dirac delta function and $\gamma_i(t)$ are the Lagrange multipliers. Multiplying both sides of (7) by $\phi(s)$ and integrating over the domain $s \in [-\tau_{\mathrm{b}}, 0)$ results in the following:

$$M_i \dot{a}_i(t) = K_i a_i(t) + \phi(0)\gamma_i(t), \quad i = 1, 2, \tag{8}$$

where $M_1 = M_2 = M$ and $K_1 = K_2 = K$ are defined as

$$M = \int_{-\tau_{\mathrm{b}}}^{0} \phi(s)\phi^{\mathrm{T}}(s)\, ds, \quad K = \int_{-\tau_{\mathrm{b}}}^{0} \phi(s)\left(\phi'(s)\right)^{\mathrm{T}}\, ds. \tag{9}$$

The Lagrange multipliers can be computed as follows [20]:

$$\gamma_i(t) = \frac{f_i}{c_3} - \frac{c_2}{c_3} a_i(t), \quad i = 1, 2, \tag{10}$$

where $c_2 = \phi^{\mathrm{T}}(0) M^{-1} K$ and $c_3 = \phi^{\mathrm{T}}(0) M^{-1} \phi(0)$. Thus, $f_i(t)$ are defined as follows, using the Galerkin projection:

$$f_1(t) = z_2(t) = \phi^{\mathrm{T}}(0) a_2(t), \tag{11a}$$
$$f_2(t) = -\beta\phi^{\mathrm{T}}(0) a_1(t) - \alpha\phi^{\mathrm{T}}(0) a_2(t) + K_{\mathrm{pb}}\phi^{\mathrm{T}}(-\tau_{\mathrm{b}}) a_1(t) + K_{\mathrm{db}}\phi^{\mathrm{T}}(-\tau_{\mathrm{b}}) a_2(t) + K_{\mathrm{ab}}\phi^{\mathrm{T}}(-\tau_{\mathrm{b}})\dot{a}_2(t). \tag{11b}$$

Note that (5) can be used to write the last term in (11b) as $K_{\mathrm{ab}}\left(\phi'(-\tau_{\mathrm{b}})\right)^{\mathrm{T}} a_2(t)$.

To obtain a system of ODEs, we proceed by first defining new variables

$$r_1 = -\beta\phi^{\mathrm{T}}(0) + K_{\mathrm{pb}}\phi^{\mathrm{T}}(-\tau_{\mathrm{b}}), \tag{12a}$$
$$r_2 = -\alpha\phi^{\mathrm{T}}(0) + K_{\mathrm{db}}\phi^{\mathrm{T}}(-\tau_{\mathrm{b}}) + K_{\mathrm{ab}}\left(\phi'(-\tau_{\mathrm{b}})\right)^{\mathrm{T}}. \tag{12b}$$

Upon substituting all obtained variables into (8), we obtain the following:

$$M\dot{a}_1(t) = (K + X_1)\, a_1(t) + X_2 a_2(t), \tag{13a}$$
$$M\dot{a}_2(t) = X_3 a_1(t) + (K + X_4)\, a_2(t), \tag{13b}$$

where

$$X_1 = -\frac{\phi(0)\phi^{\mathrm{T}}(0) M^{-1} K}{c_3}, \quad X_2 = \frac{\phi(0)\phi^{\mathrm{T}}(0)}{c_3}, \tag{14a}$$
$$X_3 = \frac{\phi(0) r_1}{c_3}, \quad X_4 = \frac{\phi(0) r_2}{c_3} - \frac{\phi(0)\phi^{\mathrm{T}}(0) M^{-1} K}{c_3}. \tag{14b}$$

Finally, we multiply (13) by $M^{-1}$ and write in matrix form as follows:

$$\dot{a}(t) = L a(t), \tag{15}$$

where $a(t) = [a_1(t), a_2(t)]^{\mathrm{T}}$ and $L$ is defined as

$$L = \begin{bmatrix} M^{-1}(K + X_1) & M^{-1} X_2 \\ M^{-1} X_3 & M^{-1}(K + X_4) \end{bmatrix}. \tag{16}$$

Equation (15) is a system of first-order ODEs whose solution approximates the solution of the original neutral DDE (1). The approximation improves as the number of modes retained in the Galerkin approximation ($N$) increases. The original system (1) is stable when all eigenvalues of $L$ have a negative real part. Stability charts can be obtained by repeating this analysis over a range of system parameters.

### C. Biomechanical Model

We augment the inverted pendulum model (Fig. 1) by introducing the following torque at the ankle joint to represent the total moment generated by the muscles:

$$T(u(t),\theta(t),\omega(t)) = u(t)T_\theta(\theta(t))T_\omega(\omega(t)), \tag{17}$$

where $\omega(t) = \dot{\theta}(t)$ and $-1 \leq u(t) \leq 1$ is the activation, with positive and negative values representing activation of the plantarflexor and dorsiflexor muscles, respectively. Moments due to passive muscle forces are assumed to be negligible over the range of motion explored in this study. We assume $u(t)$ is of the following form:

$$u(t) = \bar{K}_{\rm pb}\theta(t-\tau_{\rm b}) + \bar{K}_{\rm db}\omega(t-\tau_{\rm b}), \tag{18}$$

where $\bar{K}_{\rm pb}$ and $\bar{K}_{\rm db}$ are, respectively, the proportional and derivative control gains of the biological system and $\tau_{\rm b}$ is the reflex delay. The equation of motion is

$$\begin{aligned} J\dot{\omega}(t) - mg\ell\theta(t) = &- u(t)T_\theta^{\rm P}(\theta(t))T_\omega^{\rm P}(\omega(t)) \\ &+ u(t)T_\theta^{\rm D}(\theta(t))T_\omega^{\rm D}(\omega(t)), \end{aligned} \tag{19}$$

where $m = 60$ kg, $\ell = 1$ m, and $J = 60$ kg $\cdot$ m$^2$ are obtained from the literature [12], [28]. Superscripts P and D in (19) indicate the components of the torques generated by the plantarflexor and dorsiflexor muscles, respectively. The functions $T_\theta^{\rm P}(\theta(t))$ and $T_\theta^{\rm D}(\theta(t))$ are obtained by fitting polynomials to the curves reported by Ashby [34] over the relevant physiological range of $\pm 8^\circ$ from vertical (i.e., $|\theta(t)| \leq 0.14$ rad in Fig. 1) [36]:

$$T_\theta^{\rm P}(\theta(t)) = -1100.60\theta^2(t) + 28.25\theta(t) + 404.72, \tag{20a}$$
$$T_\theta^{\rm D}(\theta(t)) = -191.30\theta^2(t) - 107.97\theta(t) + 91.12, \tag{20b}$$

where $\theta(t)$ is expressed in radians. The function $T_\omega^{\rm P}(\omega(t))$ is defined by linearizing the relation proposed by Ashby [34]:

$$T_\omega^{\rm P}(\omega(t)) = \begin{cases} 0, & \text{if } \omega(t) > 16 \\ 1 + 0.095\omega(t), & \text{if } -5.7 \leq \omega(t) \leq 16 \\ 1.5, & \text{otherwise} \end{cases}, \tag{21}$$

where $\omega(t)$ is expressed in rad/s. Assuming $\omega(t)$ remains small during quiet stance [37], we can further simplify (21) as follows:

$$T_\omega^{\rm P}(\omega(t)) \approx 1 + 0.095\omega(t), \tag{22a}$$
$$T_\omega^{\rm D}(\omega(t)) \approx 1 - 0.095\omega(t). \tag{22b}$$

Substituting (18), (20), and (22) into (19) and dropping higher-order terms, we obtain the following equation of motion:

$$\dot{\omega}(t) = E\theta(t) - K_{\rm pb}\theta(t-\tau_{\rm b}) - K_{\rm db}\omega(t-\tau_{\rm b}), \tag{23}$$

where $E = mg\ell/J$, $K_{\rm pb} = 313.60\bar{K}_{\rm pb}/J$, and $K_{\rm db} = 313.60\bar{K}_{\rm db}/J$. In state-space form, we have

$$f_1(t) = z_2(t), \tag{24a}$$
$$f_2(t) = Ez_1(t) - K_{\rm pb}z_1(t-\tau_{\rm b}) - K_{\rm db}z_2(t-\tau_{\rm b}). \tag{24b}$$

For this system, the boundary conditions are imposed in the Galerkin approximation by defining

$$r_1 = E\phi^{\rm T}(0) - K_{\rm pb}\phi^{\rm T}(-\tau_{\rm b}), \tag{25a}$$
$$r_2 = -K_{\rm db}\phi^{\rm T}(-\tau_{\rm b}). \tag{25b}$$

As described in Section II-B, we determine the stability of the system by computing the eigenvalues of matrix $L$ (16). To determine a suitable value for $N$, we substitute $\theta(t) = e^{\lambda t}$ into (23) to obtain the characteristic function

$$-\lambda^2 + \frac{mg\ell}{J} - \frac{K_{\rm pb}}{e^{\lambda\tau_{\rm b}}} - \frac{K_{\rm db}\lambda}{e^{\lambda\tau_{\rm b}}} = 0, \tag{26}$$

which we use to compute the error in the Galerkin approximation.

### D. Exoskeleton Model

The exoskeleton is assumed to generate torques using a PD control law with delayed feedback of the angle and angular velocity of the ankle joint. The feedback delay is assumed to be different from the biological reflex delay. The exoskeleton is idealized in that it applies torques directly to the ankle joint and it is assumed to be massless. (One may also consider its mass and inertia to be lumped into the inverted pendulum model.) We obtain the following equation of motion for the system with exoskeleton assistance:

$$\begin{aligned} \dot{\omega}(t) = &\, E\theta(t) - K_{\rm pb}\theta(t-\tau_{\rm b}) - K_{\rm db}\omega(t-\tau_{\rm b}) \\ &- \frac{K_{\rm pe}\theta(t-\tau_{\rm e})}{J} - \frac{K_{\rm de}\omega(t-\tau_{\rm e})}{J}, \end{aligned} \tag{27}$$

where $K_{\rm pe}$ and $K_{\rm de}$ are, respectively, the proportional and derivative control gains of the exoskeleton and $\tau_{\rm e}$ is the exoskeleton feedback delay, which includes the time required to measure the feedback signals, the computation time, and the response time of the actuators.

## III. Results

We first use the inverted pendulum model defined in Section II-A to verify convergence of our Galerkin approximation where boundary conditions are imposed via the Lagrange multiplier method. We then consider the biomechanical model and determine the stability of the unassisted system in the space of the reflex control gains ($K_{\rm pb}$ and $K_{\rm db}$). Next, we explore the stability of the assisted system as the exoskeleton control gains ($K_{\rm pe}$ and $K_{\rm de}$) vary. Finally, we study the stability of the system over a range of delays in the biological system and exoskeleton ($\tau_{\rm b}$ and $\tau_{\rm e}$).

### A. Model Verification

The stability chart for the inverted pendulum model is shown in Fig. 2 in the parameter space of $K_{\rm pb}$ and $K_{\rm db}$, with $K_{\rm ab} = 54$. Good agreement between our Galerkin approximation and the analytical solution of Insperger et al. [12] is found when at least $N = 7$ modes are retained in the Galerkin approximation. Comparison of the rightmost eigenvalues with those reported by Ahsan et al. [28] (Table I) reveals only small differences which can be attributed to differences in the strategy used to impose the boundary conditions.

TABLE I
COMPARISON OF THE RIGHTMOST EIGENVALUES OF THE INVERTED PENDULUM MODEL USING OUR GALERKIN APPROXIMATION WITH THOSE REPORTED BY AHSAN *et al.* [28]

| Parameter | | Result | Rightmost Eigenvalues | | | |
|---|---|---|---|---|---|---|
| $K_{\mathrm{pb}}$ | $K_{\mathrm{db}}$ | | $N=3$ | $N=5$ | $N=7$ | $N=9$ |
| 1764 | 600 | Ahsan et al. | $0.69 \pm 11.71j$ | $0.70 \pm 11.21j$ | $0.70 \pm 11.21j$ | — |
| | | Section II-B | $-1.42 \pm 11.49j$ | $0.72 \pm 11.17j$ | $0.69 \pm 11.21j$ | $0.69 \pm 11.21j$ |
| 2940 | 600 | Ahsan et al. | $0.55 \pm 10.37j$ | $0.65 \pm 10.01j$ | $0.65 \pm 10.01j$ | — |
| | | Section II-B | $-1.22 \pm 9.09j$ | $0.68 \pm 9.98j$ | $0.64 \pm 10.00j$ | $0.64 \pm 10.00j$ |
| 3528 | 600 | Ahsan et al. | $0.94 \pm 9.58j$ | $1.03 \pm 9.35j$ | $1.03 \pm 9.35j$ | — |
| | | Section II-B | $-0.03 \pm 8.62j$ | $1.04 \pm 9.32j$ | $1.02 \pm 9.33j$ | $1.02 \pm 9.33j$ |

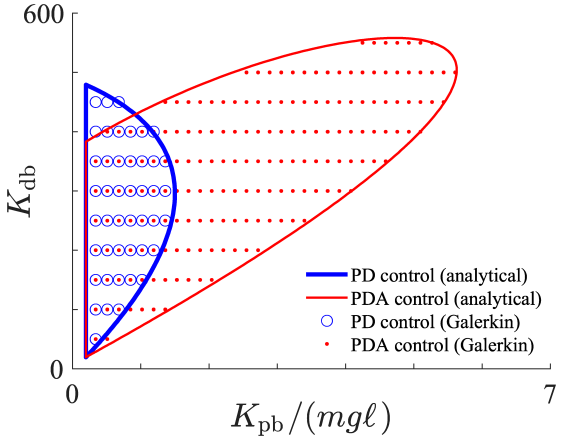


Fig. 2. Stability chart for the inverted pendulum model using our Galerkin approximation (blue circles and red dots) and the analytical solution of Insperger et al. [12] (blue and red lines).

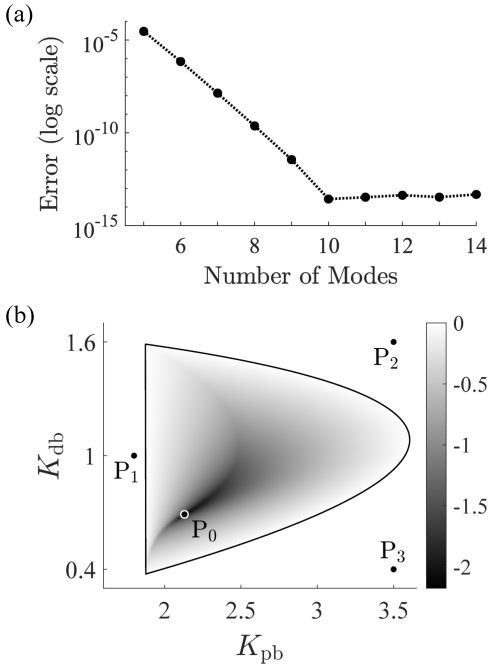


Fig. 3. Stability analysis of the unassisted biomechanical model with reflex delay $\tau_{\mathrm{b}} = 0.2$ s: (a) convergence of the Galerkin approximation with $K_{\mathrm{pb}} = 2.13$ and $K_{\mathrm{db}} = 0.69$; (b) stability chart. In panel (b), the scale and shading indicate the real part of the rightmost eigenvalue; the black line is the analytical solution of the stability boundary reported by Insperger et al. [12].

### *B. Biomechanical Model Without Assistance*

We performed a convergence analysis by setting $K_{\mathrm{pb}} = 2.13$, $K_{\mathrm{db}} = 0.69$, and $\tau_{\mathrm{b}} = 0.2$ s in (23) and substituting the rightmost eigenvalue ($\lambda$) into (26). The magnitude of the error is shown in Fig. 3(a). As shown, convergence is reached for $N = 10$ modes in the Galerkin approximation; however, to accommodate potential changes in system behaviour for different control gains and time delays, we use $N = 14$ modes in all remaining analyses.

The stability chart for the unassisted biomechanical model is shown in Fig. 3(b), again using reflex delay $\tau_{\mathrm{b}} = 0.2$ s. Regions with larger stability margins (i.e., where the rightmost eigenvalues are further away from the imaginary axis) are darker; unstable regions are white. Good agreement is observed between the results obtained using our Galerkin approximation and the analytical stability boundary [12]. Note, however, that the Galerkin approximation method can be used to determine the region of stability as well as the stability margin at each point in the stable region. In the following sections, we consider the four points labelled in Fig. 3(b). Point $P_0 = (2.13, 0.69)$ indicates the pair of biological reflex control gains resulting in the largest stability margin. The other three points represent scenarios in which the human model is unstable when unassisted: $P_1 = (1.8, 1.0)$, $P_2 = (3.5, 1.6)$, and $P_3 = (3.5, 0.4)$.

### *C. Effect of Exoskeleton Gains on Stability*

The stability of the assisted biomechanical model is shown in Fig. 4 for three exoskeleton feedback delays ($\tau_{\mathrm{e}}$), using reflex gains $P_0$ and delay $\tau_{\mathrm{b}} = 0.2$ s. We confirm that the system is stable for $K_{\mathrm{pe}} = K_{\mathrm{de}} = 0$ since the unassisted biomechanical system is stable at point $P_0$ (Fig. 3(b)). We observe that the area of the stability region increases as the exoskeleton feedback delay decreases. A smaller exoskeleton feedback delay also moves the rightmost eigenvalues further away from the imaginary axis in general. Thus, the addition of the exoskeleton improves the stability of an inherently stable biomechanical model.

The exoskeleton is also able to stabilize an inherently unstable biomechanical model. Stability charts are shown in Fig. 5 using reflex gains $P_1$, $P_2$, and $P_3$, with reflex delay

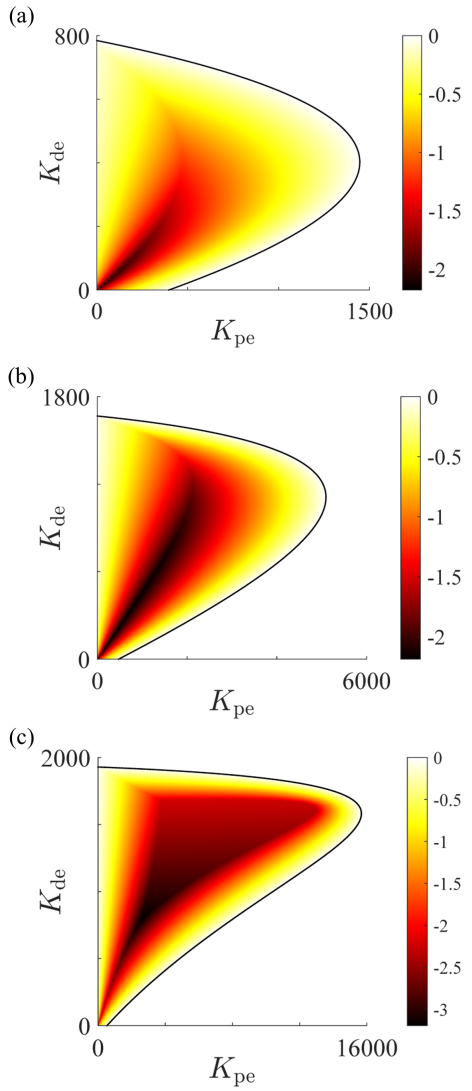


Fig. 4. Stability charts for the exoskeleton-assisted biomechanical model with reflex gains $P_0$ and delay $\tau_b = 0.2$ s: (a) $\tau_e = 0.1$ s; (b) $\tau_e = 0.067$ s; (c) $\tau_e = 0.05$ s. The scales and shading indicate the real part of the rightmost eigenvalue.

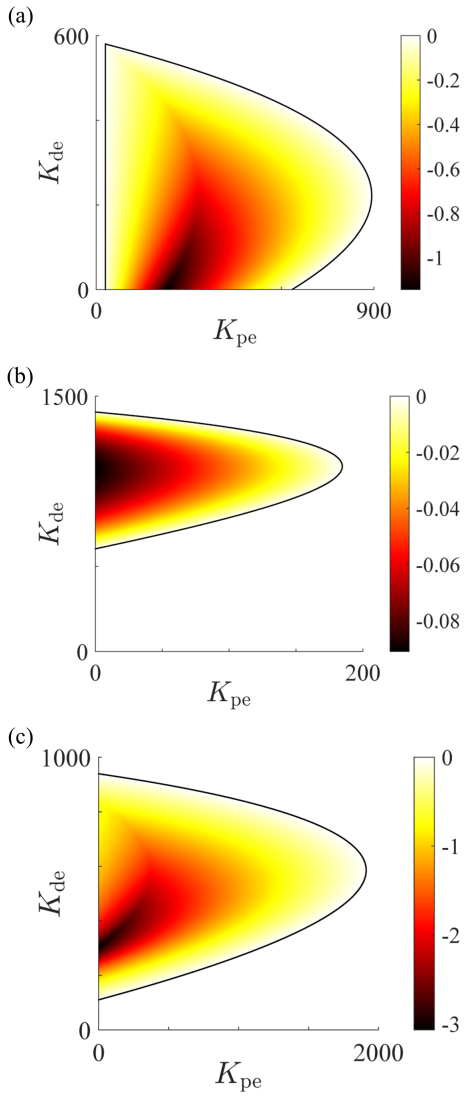


Fig. 5. Stability charts for the exoskeleton-assisted biomechanical model with delay $\tau_b = 0.2$ s: (a) reflex gains $P_1$, $\tau_e = 0.1$ s; (b) reflex gains $P_2$, $\tau_e = 0.071$ s; (c) reflex gains $P_3$, $\tau_e = 0.1$ s. The scales and shading indicate the real part of the rightmost eigenvalue.

$\tau_b = 0.2$ s. Note that, for reflex gains defined by $P_1$ and $P_3$, the exoskeleton is able to stabilize the system when the feedback delay is $\tau_e = 0.1$ s. However, at $P_2$, the assisted biomechanical model can be stabilized only for exoskeleton feedback delays up to approximately $0.071$ s.

### *D. Effect of Time Delays on Stability*

The stability boundary for four combinations of reflex delay ($\tau_b$) and exoskeleton feedback delay ($\tau_e$) are shown in Fig. 6, over a range of exoskeleton gains with reflex gains set to $P_0$. As shown, the stability boundary changes in both area and overall shape. Although other metrics may also be important, we use the area of the stability region to quantify the stability of the exoskeleton-assisted biomechanical model as the delays vary. We consider reflex delays in the range $0.075$ s $\leq \tau_b \leq 0.256$ s [7], [10], and exoskeleton delays in the range $0.055$ s $\leq \tau_e \leq 0.124$ s based on delays that have been used in the literature to be compatible with the biological reflex delay [32], [33].

The area of the stability region in the parameter space of $K_{pe}$ and $K_{de}$ is shown in Fig. 7 as the reflex and exoskeleton time delays vary. Areas were computed by generating stability regions similar to those shown in Fig. 6 and integrating the enclosed area. Note that all stability regions reside entirely within the first quadrant of the parameter space. The black circle in each panel of Fig. 7 indicates the combination of time delays resulting in the stability region with the largest area. It is important to note that the area of the stability region does not necessarily decrease as the reflex delay decreases, though a smaller exoskeleton time delay is always beneficial. For example, in Fig. 7(a), a reflex delay of $\tau_b = 0.2$ s results in a larger stability region than a reflex delay of $\tau_b = 0.1$ s when the exoskeleton delay is small.

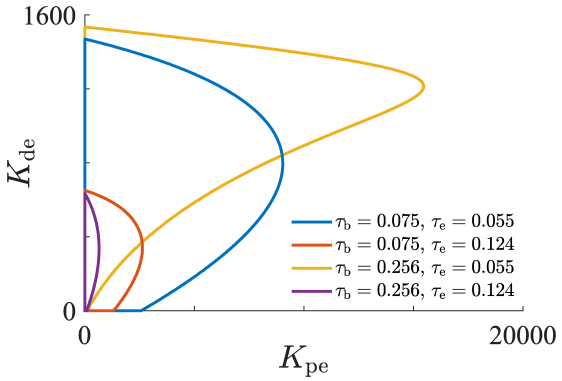


Fig. 6. Stability boundaries for the minimum and maximum reflex delays ($\tau_b$) and exoskeleton feedback delays ($\tau_e$) considered in this work, with reflex gains $P_0$.

## IV. Conclusions

The stability of postural sway during quiet stance was studied using an inverted pendulum model, considering reflex delays in the biomechanical system as well as feedback delays in the exoskeleton controller. We used the Galerkin projection method to translate the governing second-order neutral DDE into a system of first-order ODEs. The eigenvalues of the ODE system could then be readily computed to quantify the stability of the original DDE system. We verified our modelling approach through comparison to stability boundaries reported in the literature using a simple actuator at the ankle. We then introduced a torque at the ankle that reflects the moment-generating capability of the plantarflexor and dorsiflexor muscles, and further augmented the system by adding an exoskeleton torque under PD control with delayed feedback. Using the Galerkin method, we obtained not only the stability boundaries but also the stability margin as gains and time delays varied. The three key findings from this study were as follows: (1) the modelled assistive device was capable of stabilizing inherently unstable human models; (2) with knowledge of the biological system parameters, the proposed strategy can be used to estimate the maximum exoskeleton delay that will stabilize the system; and (3) in some scenarios, reducing the reflex delay will decrease the area of the stability region.

There are several limitations of this study. First, we have used a simple inverted pendulum model which neglects motion of the knee, hip, and upper body, as well as motion in the frontal plane. Second, we have approximated the torques generated by all plantarflexor and dorsiflexor muscles using two actuators, and we have not modelled muscle force-generation delays. Third, we have limited our analysis to PD-controlled exoskeletons. Finally, our simulation results have not been validated with experiments.

Exoskeletons and other active assistive devices represent a substantial opportunity to improve health and longevity. Study of the physical and neurological interfaces between biological and mechatronic systems will lead to improved device designs and fewer injuries. The proposed modelling and simulation approach can provide insight into the effect of changes in the magnitude and timing of muscle reflexes and assistive torques on postural stability. These simulations provide valuable insight by isolating parameters that cannot be controlled in experiments. Although the exoskeleton designer

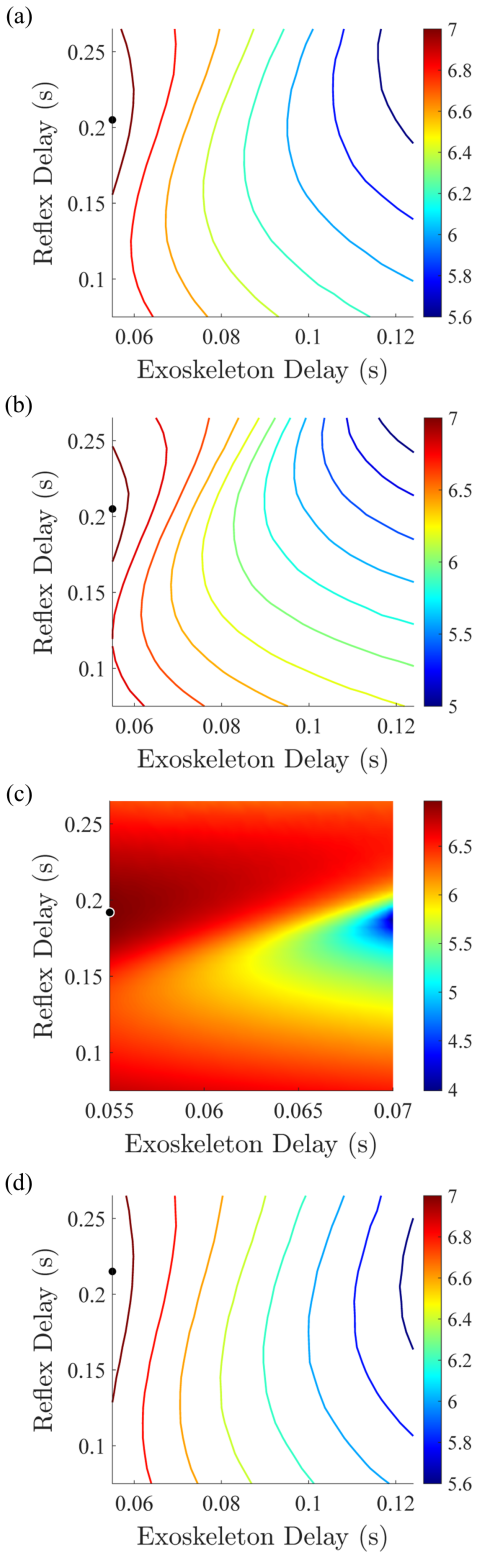


Fig. 7. Logarithm of the area of the stability region in the space of the exoskeleton control gains: (a) reflex gains $P_0$; (b) reflex gains $P_1$; (c) reflex gains $P_2$; (d) reflex gains $P_3$. The black circle indicates the stability region with largest area.

cannot control the inherent gains and reflex delays of the biological system, these model parameters could be measured or identified over time to improve exoskeleton performance. Future work includes applying these modelling and simulation techniques to more detailed biological models (e.g., applying forces along individual muscle paths and considering muscle force-generation delays [38]), exploring the effect of exoskeleton inertia, investigating more complex exoskeleton control strategies, studying robustness in greater detail, and validating the simulation results experimentally.

## ACKNOWLEDGMENT

The authors thank C. P. Vyasarayani for sharing his expertise on delay differential equations.

## REFERENCES

[1] J. A. Stevens and E. D. Sogolow, "Gender differences for non-fatal unintentional fall related injuries among older adults," *Inj. Prev.*, vol. 11, no. 2, pp. 115–119, 2005.

[2] United Nations, Department of Economic and Social Affairs, Population Division, "World population prospects 2022: Summary of results," UN DESA/POP/2022/TR/NO. 3, Tech. Rep., 2022.

[3] D. Sale, J. Quinlan, E. Marsh, and A. J. McComas, "Influence of joint position on ankle plantarflexion in humans," *J. Appl. Physiol.*, vol. 52, no. 6, pp. 1636–1642, 1982.

[4] E. Marsh, D. Sale, A. J. McComas, and J. Quinlan, "Influence of joint position on ankle dorsiflexion in humans," *J. Appl. Physiol.*, vol. 51, no. 1, pp. 160–167, 1981.

[5] S.-K. Bok, T. H. Lee, and S. S. Lee, "The effects of changes of ankle strength and range of motion according to aging on balance," *Ann. Rehabil. Med.*, vol. 37, no. 1, pp. 10–16, 2013.

[6] A. H. Vette, K. Masani, and M. R. Popovic, "Time delay from muscle activation to torque generation during quiet stance: implications for closed-loop control via FES," in *Proc. 13th Annu. Conf. Int. FES Soc.*, Freiburg, Germany, September 21–25, 2008, pp. 423–425.

[7] R. J. Peterka, "Sensorimotor integration in human postural control," *J. Neurophysiol.*, vol. 88, no. 3, pp. 1097–1118, 2002.

[8] A. D. Kuo, "An optimal control model for analyzing human postural balance," *IEEE Trans. Biomed. Eng.*, vol. 42, no. 1, pp. 87–101, 1995.

[9] B. W. Verdaasdonk, H. F. J. M. Koopman, S. A. van Gils, and F. C. T. van der Helm, "Bifurcation and stability analysis in musculoskeletal systems: a study in human stance," *Biol. Cybern.*, vol. 91, no. 1, pp. 48–62, 2004.

[10] K. Masani, A. H. Vette, and M. R. Popovic, "Controlling balance during quiet standing: proportional and derivative controller generates preceding motor command to body sway position observed in experiments," *Gait Posture*, vol. 23, no. 2, pp. 164–172, 2006.

[11] Y. Asai, Y. Tasaka, K. Nomura, T. Nomura, M. Casadio, and P. Morasso, "A model of postural control in quiet standing: robust compensation of delay-induced instability using intermittent activation of feedback control," *PLoS One*, vol. 4, no. 7, p. e6169, 2009.

[12] T. Insperger, J. Milton, and G. Stépán, "Acceleration feedback improves balancing against reflex delay," *J. R. Soc. Interface*, vol. 10, no. 79, p. 20120763, 2013.

[13] T. Insperger and J. Milton, *Delay and Uncertainty in Human Balancing Tasks*. Cham, Switzerland: Springer, 2021.

[14] T. Balogh, B. Varszegi, and T. Insperger, "On the admissible control-loop delay for the inverted pendulum subject to detuned PDA feedback," *J. Sound Vib.*, vol. 529, p. 116898, 2022.

[15] A. Zelei, J. Milton, G. Stepan, and T. Insperger, "Response to perturbation during quiet standing resembles delayed state feedback optimized for performance and robustness," *Sci. Rep.*, vol. 11, no. 1, p. 11392, 2021.

[16] J. Milton, J. L. Cabrera, T. Ohira, S. Tajima, Y. Tonosaki, C. W. Eurich, and S. A. Campbell, "The time-delayed inverted pendulum: implications for human balance control," *Chaos*, vol. 19, no. 2, p. 026110, 2009.

[17] H.-Y. Huang, I. Farkhatdinov, A. Arami, and E. Burdet, "Modelling neuromuscular function of SCI patients in balancing," in *Converging Clinical and Engineering Research on Neurorehabilitation II*, J. Ibáñez, J. González-Vargas, J. M. Azorín, M. Akay, and J. L. Pons, Eds. Cham, Switzerland: Springer, 2017, pp. 355–359.

[18] A. Emmens, E. van Asseldonk, M. Masciullo, M. Arquilla, I. Pisotta, N. L. Tagliamonte, F. Tamburella, M. Molinari, and H. van der Kooij, "Improving the standing balance of paraplegics through the use of a wearable exoskeleton," in *Proc. 7th IEEE Int. Conf. Biomed. Robot. Biomechatron.*, Enschede, The Netherlands, August 26–29, 2018, pp. 707–712.

[19] K. Kaminishi, D. Li, R. Chiba, K. Takakusaki, M. Mukaino, and J. Ota, "Characterization of postural control in post-stroke patients by musculoskeletal simulation," *J. Robot. Mechatron.*, vol. 34, no. 6, pp. 1451–1462, 2022.

[20] C. P. Vyasarayani, "Galerkin approximations for neutral delay differential equations," *J. Comput. Nonlinear Dyn.*, vol. 8, no. 2, p. 021014, 2013.

[21] ——, "Galerkin approximations for higher order delay differential equations," *J. Comput. Nonlinear Dyn.*, vol. 7, no. 3, p. 031004, 2012.

[22] S. S. Kandala, T. K. Uchida, and C. P. Vyasarayani, "Pole placement for time-delayed systems using Galerkin approximations," *J. Dyn. Syst. Meas. Control*, vol. 141, no. 5, p. 051012, 2019.

[23] S. S. Kandala, S. Chakraborty, T. K. Uchida, and C. P. Vyasarayani, "Hybrid method-of-receptances and optimization-based technique for pole placement in time-delayed systems," *Int. J. Dyn. Control*, vol. 8, no. 2, pp. 558–569, 2020.

[24] S. S. Kandala, S. Samukham, T. K. Uchida, and C. P. Vyasarayani, "Spurious roots of delay differential equations using Galerkin approximations," *J. Vib. Control*, vol. 26, no. 15–16, pp. 1178–1184, 2020.

[25] Z. Ahsan, T. Uchida, and C. P. Vyasarayani, "Galerkin approximations with embedded boundary conditions for retarded delay differential equations," *Math. Comput. Model. Dyn. Syst.*, vol. 21, no. 6, pp. 560–572, 2015.

[26] A. Sadath and C. P. Vyasarayani, "Galerkin approximations for stability of delay differential equations with time periodic coefficients," *J. Comput. Nonlinear Dyn.*, vol. 10, no. 2, p. 021011, 2015.

[27] Z. Ahsan, A. Sadath, T. K. Uchida, and C. P. Vyasarayani, "Galerkin–Arnoldi algorithm for stability analysis of time-periodic delay differential equations," *Nonlinear Dyn.*, vol. 82, no. 4, pp. 1893–1904, 2015.

[28] Z. Ahsan, T. K. Uchida, A. Subudhi, and C. P. Vyasarayani, "Stability of human balance with reflex delays using Galerkin approximations," *J. Comput. Nonlinear Dyn.*, vol. 11, no. 4, p. 041009, 2016.

[29] D. G. Thelen, "Adjustment of muscle mechanics model parameters to simulate dynamic contractions in older adults," *J. Biomech. Eng.*, vol. 125, no. 1, pp. 70–77, 2003.

[30] J. H. J. Allum, M. G. Carpenter, F. Honegger, A. L. Adkin, and B. R. Bloem, "Age-dependent variations in the directional sensitivity of balance corrections and compensatory arm movements in man," *J. Physiol.*, vol. 542, no. 2, pp. 643–663, 2002.

[31] K. Kong and D. Jeon, "Design and control of an exoskeleton for the elderly and patients," *IEEE ASME Trans. Mechatron.*, vol. 11, no. 4, pp. 428–432, 2006.

[32] M. Ding, M. Nagashima, S.-G. Cho, J. Takamatsu, and T. Ogasawara, "Control of walking assist exoskeleton with time-delay based on the prediction of plantar force," *IEEE Access*, vol. 8, pp. 138 642–138 651, 2020.

[33] I. Farkhatdinov, J. Ebert, G. van Oort, M. Vlutters, E. van Asseldonk, and E. Burdet, "Assisting human balance in standing with a robotic exoskeleton," *IEEE Robot. Autom. Lett.*, vol. 4, no. 2, pp. 414–421, 2019.

[34] B. M. Ashby, "Coordination of upper and lower limbs in the standing long jump: kinematics, dynamics, and optimal control," Ph.D. dissertation, Stanford Univ., 2004.

[35] B. M. Ashby and S. L. Delp, "Optimal control simulations reveal mechanisms by which arm movement improves standing long jump performance," *J. Biomech.*, vol. 39, no. 9, pp. 1726–1734, 2006.

[36] F. Antritter, F. Scholz, G. Hettich, and T. Mergner, "Stability analysis of human stance control from the system theoretic point of view," in *Proc. 2014 Eur. Control Conf. (ECC)*, Strasbourg, France, June 24–27, 2014, pp. 1849–1855.

[37] T. Mergner, "A neurological view on reactive human stance control," *Annu. Rev. Control*, vol. 34, no. 2, pp. 177–198, 2010.

[38] K. Masani, A. H. Vette, N. Kawashima, and M. R. Popovic, "Neuromusculoskeletal torque-generation process has a large destabilizing effect on the control mechanism of quiet standing," *J. Neurophysiol.*, vol. 100, no. 3, pp. 1465–1475, 2008.